eNeuro

Research Article: New Research | Development

Hepatocyte Growth Factor modulates MET receptor tyrosine kinase and #-catenin functional interactions to enhance synapse formation

MET signaling in synapse formation

Zhihui Xie[1], Kathie L. Eagleson[1], Hsiao-Huei Wu[1] and Pat Levitt[2]

[1]*Department of Pediatrics, The Saban Research Institute, Children's Hospital Los Angeles, Keck School of Medicine, University of Southern California, Los Angeles, CA, 90027*

[2]*Institute for the Developing Mind, The Saban Research Institute, Children's Hospital Los Angeles, Keck School of Medicine, University of Southern California, Los Angeles, CA, 90027*

DOI: 10.1523/ENEURO.0074-16.2016

Received: 5 April 2016

Revised: 19 July 2016

Accepted: 25 July 2016

Published: 1 August 2016

Author contributions: Z.X., K.E., and P.L. designed research; Z.X. and H.-H.W. performed research; Z.X., K.E., and P.L. analyzed data; Z.X., K.E., H.-H.W., and P.L. wrote the paper.

Funding: National Institute of Mental Health
MH067842

Funding: The Simms/Mann Chair in Developmental Neurogenetics

Conflict of Interest: Authors report no conflict of interest.

National Institute of Mental Health [MH067842]; The Simms/Mann Chair in Developmental Neurogenetics.

Correspondence should be addressed to Pat Levitt, PhD, The Saban Research Institute, Children's Hospital Los Angeles, 4650 Sunset Blvd, MS #135, Los Angeles, CA 90027, plevitt@med.usc.edu

Cite as: eNeuro 2016; 10.1523/ENEURO.0074-16.2016

Hepatocyte Growth Factor modulates MET receptor tyrosine kinase and β-catenin functional interactions to enhance synapse formation

Abbreviated title: MET signaling in synapse formation

Zhihui Xie[1], Kathie L. Eagleson[1], Hsiao-Huei Wu[1] and Pat Levitt[2]

[1]Department of Pediatrics and [2]Institute for the Developing Mind, The Saban Research Institute, Children's Hospital Los Angeles, Keck School of Medicine, University of Southern California, Los Angeles, CA, 90027

Corresponding Author:

Pat Levitt, PhD

The Saban Research Institute

Children's Hospital Los Angeles

4650 Sunset Blvd, MS #135

Los Angeles, CA 90027

plevitt@med.usc.edu

Author contributions: ZX and PL conceived the project, ZX, KL and PL designed experiments and analyzed data, ZX and HHW performed experiments and all people participated in writing and editing the manuscript.

Number of pages: 45; number of figures: 6; number of table: 1; number of words: Abstract, 248; Significance Statement: 93; Introduction, 628; Discussion, 1494.

Acknowledgments: This work is supported by a National Institute of Mental Health (NIMH) grant MH067842 and the Simms/Mann Chair in Developmental Neurogenetics (P.L.). The authors declare no competing financial interests.

Abstract

MET, a pleiotropic receptor tyrosine kinase implicated in autism risk, influences multiple neurodevelopmental processes. There is a knowledge gap, however, in the molecular mechanism through which MET mediates developmental events related to disorder risk. In the neocortex, MET is expressed transiently during periods of peak dendritic outgrowth and synaptogenesis, with expression enriched at developing synapses, consistent with demonstrated roles in dendritic morphogenesis, modulation of spine volume and excitatory synapse development. In a recent co-immunoprecipitation (Co-IP)/mass spectrometry screen, β-catenin was identified as part of the MET interactome in developing neocortical synaptosomes. Here, we investigated the influence of the MET/β-catenin complex in mouse neocortical synaptogenesis. Western blot analysis confirms that MET and β-catenin co-immunoprecipitate, but N-cadherin is not associated with the MET complex. Following stimulation with hepatocyte growth factor (HGF), β-catenin is phosphorylated at tyrosine^{142} (Y142) and dissociates from MET, accompanied by an increase in β-catenin/N-cadherin and MET/synapsin 1 protein complexes. In neocortical neurons in vitro, proximity ligation assays confirmed close proximity of these proteins. Moreover, in neurons transfected with synaptophysin-GFP, HGF stimulation increases the density of synaptophysin/bassoon (a presynaptic marker) and synaptophysin/PSD95 (a postsynaptic marker) clusters. Mutation of β-catenin at Y142 disrupts the dissociation of the MET/β-catenin complex and prevents the increase in clusters in response to HGF. The data demonstrate a new mechanism for modulation of synapse formation, whereby MET activation induces an alignment of pre- and

postsynaptic elements that are necessary for assembly and formation of functional synapses by subsets of neocortical neurons that express MET/β-catenin complex.

Keywords: MET receptor tyrosine kinase, β-catenin, synapse development, autism

Significance Statement

The gene encoding the MET receptor tyrosine kinase is associated with autism spectrum disorder, and influences typical and atypical synapse development and cortical circuit function. The present studies focus on determining potential molecular mechanisms through which the receptor functions in neocortical neurons during synaptogenesis. The findings show that the MET receptor interacts functionally with other proteins also implicated in promoting new synapse assembly, which is reduced upon disruption of the interactions. Thus, in some instances of autism spectrum disorder, disturbances of these molecular interactions may relate to the pathophysiology of cortical circuit development.

Introduction

The MET receptor tyrosine kinase has been implicated in multiple neurodevelopmental processes (Peng et al., 2013) and thus outcomes from disruptions in MET function vary according to cell context. For example, in the forebrain, a risk allele for autism spectrum disorder (ASD) in the *MET* promoter, which reduces *MET* transcript and protein levels (Campbell et al., 2006; Campbell et al., 2007), is correlated with altered circuit function in typical and ASD human populations (Rudie et al., 2012) and in gray matter growth (Hedrick et al., 2012). Further, following conditional deletion of *Met* in mice, there is an increase in local interlaminar drive onto layer V neurons in the neocortex and premature maturation of excitatory synapse function in the hippocampus (Qiu et al., 2011; Qiu et al., 2014). Analyses in vivo and in vitro demonstrate that MET signaling modulates dendritic morphogenesis, spine volume, the clustering of postsynaptic proteins, excitatory synapse formation and maturation in the neocortex, striatum and hippocampus (Gutierrez et al., 2004; Tyndall and Walikonis, 2006; Nakano et al., 2007; Lim and Walikonis, 2008; Judson et al., 2010; Finsterwald and Martin, 2011; Qiu et al., 2011; Kawas et al., 2013; Qiu et al., 2014; Eagleson et al., 2016; Peng et al., 2016). These developmental influences likely underlie the mature forebrain circuit phenotypes observed in the context of altered MET signaling. How MET receptor activation mediates these discrete cellular outcomes is only beginning to be addressed, with most focus on the diversity of downstream signaling pathways initiated following activation of MET (Finsterwald and Martin, 2011; Eagleson et al., 2016). Evidence from cell lines, however, indicates that the repertoire of MET protein-interacting partners expressed by a cell also can modulate MET signaling to influence biological outcomes (Smyth and

87 Brady, 2005; Wang et al., 2005; Zeng et al., 2006; Reshetnikova et al., 2007; DeAngelis
88 et al., 2010; Bozkaya et al., 2012; Burghy et al., 2012; Lu et al., 2012; Niland et al.,
89 2013). A recent co-immunoprecipitation/mass spectrometry (Co-IP/MS) study identified
90 the MET interactome with 72 proteins, including β-catenin, in isolated murine neocortical
91 synaptosomes during the peak of synaptogenesis (Xie et al., 2016).
92
93 In the current study, we focused on the role of the MET/β-catenin protein
94 complex in HGF-mediated neocortical synapse formation. Previous studies have shown
95 that: 1) MET and β-catenin are expressed at the developing neocortical synapse
96 (Phillips et al., 2001; Murase et al., 2002; Eagleson et al., 2013); 2) MET activation
97 increases synapse density on neocortical neurons in vitro (Eagleson et al., 2016); 3) β-
98 catenin regulates synaptic vesicle localization during presynaptic development in the
99 hippocampus (Bamji et al., 2003; Yu and Malenka, 2003); and 4) functional interactions
100 between MET and β-catenin can be observed in hippocampal neurons, as well as
101 cancer cell lines (Monga et al., 2002; Herynk et al., 2003; David et al., 2008), with the
102 stability of the complex dependent upon the presence of hepatocyte growth factor
103 (HGF). MET and β-catenin physically interact with each other *in vitro*, and the activated
104 MET receptor directly phosphorylates β-catenin at tyrosine^{142} (Y142) (David et al.,
105 2008). Consistently, following addition of HGF in hippocampal neurons, β-catenin is
106 phosphorylated at Y142 and dissociates from MET (Herynk et al., 2003; Rasola et al.,
107 2007; David et al., 2008; Bhardwaj et al., 2013). Here, we used Co-IP/Western blot,
108 proximity ligation assays and immunocytochemical analyses to determine how the
109 MET/β-catenin complex might modulate neocortical synapse development in response

to HGF. We report, following stimulation with HGF, a dynamic regulation of MET-β-catenin- and MET-synapsin 1-containing complexes in synaptosomes and within minutes, a rapid increase in synapses in primary cultures of neocortical neurons. Both outcomes are dependent upon phosphorylation of β-catenin at Y142. We propose a model in which an axis of HGF/MET/β-catenin signaling modulates neocortical synapse development. Disruption of this signaling complex may contribute to ASD etiology.

Materials and Methods

Mice

Timed-pregnant C57BL/6^{J} mice were purchased from the Jackson Laboratory and the day of birth was considered postnatal day (P) 0. Animals had free access to food and water and were housed in a 13:11 (light:dark) cycle. All research procedures using mice were approved by the Institutional Animal Care and Use Committee at Children's Hospital Los Angeles. All efforts were made to minimize animal suffering and to reduce the number of animals used.

Plasmid construction

Mouse β-catenin full-length cDNA was cloned by PCR from an adult mouse brain cDNA library using high proof PfuUltra II Fusion HS DNA Polymerase (Agilent) according to the manufacturer's protocol, using the following primer pair: 5' CTAGCTAGCTAGATGGATACGTATCGCTACATAATGGCTACTCAAGC 3' and 5' TGCTCTAGAGCATTACAGGTCAGTATCAAACCAGGCCAGCTGATT 3'. Purified β-catenin cDNA fragments were subcloned into a PCI expression vector (Promega) and transformed into DH5α competent cells (Invitrogen). PCI-β-catenin plasmids were purified using the Zyppy™ plasmid maxiprep kit (Zymo Research) and PCR site-directed mutagenesis of β-catenin (β-catenin Y142F) performed according to a published strategy (Zheng et al., 2004) using the following primer pair: 5' GTTGTCAATTTGATTAACTTCCAGGATGACGCGGAACTTG 3' and 5' CAAGTTCCGCGTCATCCTGGAAGTTAATCAAATTGACAAC 3'. The β-catenin and β-catenin Y142F fragments were PCR amplified using the following primer pair:

5’ CGGGATCCATGGATACGTATCGCTACATAATGGCTACTCAAGC 3’ and
5’ CGGGATCCTTACAGGTCAGTATCAAACCAGGCCAGCTGATT 3'.
The purified fragments were subcloned into a p3XFLAG-CMV-10 vector (Sigma) to generate p3XFLAG-CMV-10-β-catenin and p3XFLAG-CMV-10-β-cateninY142F plasmids. The fidelity of the entire coding sequences of all plasmids was confirmed by DNA sequencing (Genewiz, Inc.).

RNAscope

P14 mouse brains were fresh-frozen in ice-cold isopentane and sectioned in the coronal plane at 25 μm. Sections were subjected to dual fluorescent in situ hybridization using the RNAscope Multiplex Fluorescent Reagent kit (Advanced Cell Diagnostics) according to manufacturer’s instructions. RNAscope probes and the regions used to generate the probes were: *Met* (accession # NM_008591.2 region 3370-4286, cat # 405301-C2) and *β-catenin* (accession# NM_007614.3 region 342-2511, cat # 311741). Alexa488 and Atto550 detection reagents were used to visualize *Met* and *β-catenin*, respectively. Images were acquired using a Zeiss LSM 710 confocal microscope (Zeiss) with a 20x objective. The imaging parameters and Z-axis was adjusted to bring the sample into focus. The parameters were maintained to capture focused optical images in each wavelength.

Co-IP and Western blot analysis

All reagents for Co-IP and Western blots were from Sigma, unless otherwise noted. Crude synaptosomes were isolated from the neocortex of male and female P14 mice

(Judson et al., 2010) and resuspended in sodium bicarbonate-buffered oxygenated artificial cerebrospinal fluid (ACSF - NaCl (12.4mM), KCl (0.4mM), KH_2PO_4 (0.1mM, Baker), $CaCl_2$ (0.25mM, Baker), $MgCl_2$ (0.1mM), Dextrose (1mM, VWR)). Either 25 ng/ml HGF (R&D systems) or the same volume of vehicle (phosphate buffered saline, PBS) was added for 5 minutes (Co-IP experiments) or for 5, 10, 20 minutes (β-catenin phosphorylation experiment) at 37°C to the synaptosomes. For Co-IP experiments, the synaptosomes were centrifuged at 16000 g for 15 minutes and the pellets were lysed in Co-IP lysis buffer containing 50mM HEPES pH 7.4, 2mM EGTA, 2mM EDTA, 30mM NaF, 10mM sodium orthovanadate, 40mM Beta-Glycerol phosphate, 1% Trixton-X100, and protease inhibitor cocktail. The lysate was centrifuged at 16000 g for 30 minutes and the resulting supernatant used for Co-IP, with a goat anti-MET antibody (R&D Systems), a mouse anti-β-catenin antibody (BD Biosciences) or a rabbit anti-N-cadherin antibody (Santa Cruz Biotechnology). An equivalent amount of goat, mouse or rabbit IgG antibody (Jackson ImmunoResearch) was used in parallel lysates as a negative control. The Co-IP complexes were bound to protein G agarose beads (Pierce), after which the beads were washed in Co-IP lysis buffer plus 150mM NaCl. The complexes were eluted from the beads by boiling in final sample buffer (12.5mM Tris-HCl, pH 6.8, 5% Glycerol, 5mL, 0.4% SDS, 1% 2-mercaptoethanol, 0.02% bromophenol blue) and analyzed by Western blot. For the β-catenin phosphorylation experiment, the synaptosomes were centrifuged at 16000 g for 15 minutes followed by lysis in final sample buffer. Blots were probed with antibodies directed against β-catenin (BD biosciences, 1:2000), N-cadherin (Santa Cruz Biotechnology, 1:500), synapsin1 (EMD Millipore, 1:4000), synaptophysin1 (EMD Millipore, 1:2000), phospho-MET (Cell

Signaling, 1:500) and MET (Santa Cruz, 1:500). Digital images of the Western blots were acquired using a CCD camera coupled to a UVP BioImaging System using VisionWorksLS Image Acquisition software (v8.0, UVP).

Semi-quantification of the Co-IPs

Western blot analyses of Co-IPs in neocortical synaptosomes in the presence or absence of HGF were performed in three independent experiments. For each blot, representing an independent Co-IP experiment, the density of each immunoreactive band was measured in ImageJ (version 1.46r) and a background subtraction was applied. First, to account for different efficiencies of each pull down in each experiment, a ratio of co-immunoprecipitated protein (e.g. β-catenin in Figure 1A) to immunoprecipitated protein (e.g. MET in Figure 1A) was generated. Then, for each candidate, the data are expressed as the fold-change levels in the HGF-treated group compared to the PBS-treated group. The data are presented as box plots using GraphPad Prism 6.

Primary neocortical neuron cultures

Primary cultures of neocortical neurons were prepared from P1 mice (Beaudoin et al., 2012) with the following minor modifications. In each culturing session, tissue from 2 male and female pups was pooled and approximately 50,000 cells/cm^2 were seeded onto 12 mm coverslips (Carolina Biological Supply Company) in 24-well plates, which were precoated with poly-D-lysine (Sigma). Cells were initially plated in Dulbecco's Modified Eagle's Medium (Invitrogen) supplemented with 10% fetal bovine serum

(FBS). After 4 hours, the medium was replaced with neurobasal medium (Invitrogen) supplemented with B27 (Invitrogen) and L-glutamine (Invitrogen), and one-half of the volume of medium was replaced every 3 days. This condition results in slower growth than when using glial conditioned medium or a glial feeder layer. To achieve sparse labeling of neurons, at 5 days in vitro (DIV), cultures were transfected with a p3XFLAG-CMV10-β-catenin or p3XFLAG-CMV10-β-catenin Y142F vector using a calcium phosphate transfection kit according to manufacturer's instructions (Clontech). In some experiments, a synaptophysin-GFP (Syn-GFP) plasmid (obtained from L. Reichardt, University of California, San Francisco) was co-transfected to label synaptic vesicles. At 14 DIV, 25 ng/ml HGF or the same volume of PBS was added to the medium for 5, 10 or 30 minutes (proximity ligation assays, PLA) or for 10 minutes (Syn-GFP cluster assays). The experiments were repeated in at least three independent culturing sessions. At the end of the assay period, coverslips were fixed with 4% paraformaldehyde for 15 minutes at room temperature, and processed for immunocytochemistry.

The PLA assay was used to determine spatial proximity between proteins that are immunolabeled with the Duolink in situ PLA kit (Sigma), as described previously (Eagleson et al., 2013). Immunoflurescent signals using dual imaging channels represent proteins that are within 40nm or less of each other. The following antibody combinations were used: α-MET (R&D systems, 1:50) with 1) α-β-catenin (BD biosciences, 1:50), 2) α-synapsin1 (EMD Millipore, 1:100), or 3) α-flag (Sigma, 1:200). For the Syn-GFP cluster assays, coverslips were incubated with pre-chilled 100%

methanol for 10 minutes at 4°C, then permeabilized with 0.1% Triton-X100 in PBS (PBST) for 20 minutes and blocked in blocking buffer (5% FBS in PBST) for 1 hour at room temperature. Coverslips were incubated overnight at 4°C in the following primary antibody cocktails diluted in blocking buffer: 1) rabbit anti-bassoon (Cell Signaling, 1:500) and mouse anti-flag (Sigma, 1:1000), or 2) mouse anti-PSD95 (Thermo Scientific, 1:1000) and rabbit anti-flag (1:1000). Following three washes with PBS, coverslips were incubated for 1 hour at room temperature in the following cocktails of Alexa Fluor-labeled secondary antibodies (Life Technologies, all at 1:1000): 1) 546-goat-anti-mouse and 633-goat-anti-rabbit for bassoon/flag staining, or 2) 546 goat anti-rabbit and 633-goat-anti-mouse for PSD95/flag staining. After 3 washes in PBS, coverslips were mounted onto glass slides with Prolong mounting medium (Life Technologies).

Image analysis

Images were captured using an automated laser scanning confocal microscope (Zeiss LSM 710) with a 60x oil immersion objective. The focal point of the beam and the Z-axis were adjusted until an appropriate focus was reached. All images in a given culturing session were captured and analyzed with the same exposure time and settings. Note that visualization of spines requires a longer exposure than that needed to visualize labeling of synaptic proteins in the linear range. Because the settings were optimized for analysis of synapses, there is an apparent absence of dendritic protrusions in the captured images. For PLA analyses, in each culturing session, 6-8 fields were randomly imaged for each treatment group. Quantitative measures of MET association with select

protein partners were obtained by counts of PLA clusters/area of dendrite using published methods (Eagleson et al., 2013). For the Syn-GFP cluster assays, axons from 8 transfected neurons, based on Syn-GFP labeling, were imaged for each treatment group in each culturing session. Images were imported into ImageJ (NIH) for analysis. Syn-GFP puncta co-labeled with bassoon or PSD95, and single-labeled Syn-GFP puncta, were identified using an automated plugin to Image J [https://github.com/Pat-Levitt/SynapseCounter; (Wang et al., 2015)], with thresholds set in each channel independently. Once the threshold was set for a given culturing session, the same threshold was used throughout the analyses. The following parameters were then measured for each co-labeled Syn-GFP-positive puncta using the "analyze particles" tool: 1) density (average number of puncta per 100 µm of axon length), 2) integrated density (the product of the puncta area and the average gray value within that area), 3) major length (the length of the major axis of Syn-GFP fluorescence signal expressed as average Feret's diameter), and 4) size of the puncta.

Statistics

Data were expressed as the mean ± SEM. For each experimental manipulation, data were collected from at least three independent culturing sessions. Individual neurons were considered as samples (Sun and Bamji, 2011; Crowell et al., 2015) and sample size varied between studies and is indicated in the figure legends. The normality of the data was tested using the D'Agostino & Pearson omnibus normality test. If the data were not normally distributed, either the data were transformed to meet the assumption of normal distribution or a nonparametric test was applied. Specifically, the data in

Figures 1F, 4D and 6C were transformed with square root and the data in Figure 6D were transformed with natural logarithm to meet the assumption of normality for two-way ANOVA analyses. For two-way ANOVA analyses, means were compared to determine the effects of treatment (PBS and HGF) x treatment time, or treatment x transfected plasmid (wild type β-catenin and β-catenin-Y142F), and the interaction between those factors. If a significant effect was detected, a Bonferroni's multiple comparisons test was performed to determine the possible source of interactions. When the data were not normally distributed, the Mann-Whitney U test was used to compare differences between PBS and HGF-treated groups. The unpaired t test with Welch's correction was applied to compare differences between PBS and HGF-treated groups if the data were normally distributed. For all tests, p values are reported to the fourth decimal place and values < 0.05 considered significant. Statistical analyses and preparation of graphs were performed using GraphPad Prism 6.0.

Results

HGF down-regulates the MET and β-catenin complex during synapse development

Previously, a discovery-based Co-IP/MS method was used to detect the MET interactome in neocortical synaptosomes at the peak of synaptogenesis (P14), and identified β-catenin as a member of the MET interactome (Xie et al., 2016). In this study, we took several approaches to validate and characterize the functional relevance of the MET/β-catenin complex. First, we confirmed the presence of a MET/β-catenin complex in neocortical crude synaptosomes using Western blot analysis of Co-IPs. Specifically, β-catenin was detected in MET-immunoprecipitated complexes (Figure 1A) and, conversely, MET was present in β-catenin-immunoprecipitated complexes (Figure 1B). Neither protein was detected in complexes that had been immunoprecipitated with control IgG. Activation of the MET receptor following treatment of the synaptosomes with HGF for 5 minutes was accompanied by a significant decrease in MET/β-catenin complex (mean fold change (HGF/PBS): 0.3987, 95% CI: [0.0773, 0.7201] for β-catenin in MET IP; mean fold change (HGF/PBS): 0.3760, 95% CI: [0.0606, 0.6915] for □□□ in β-catenin IP; Figure 1D). The β-catenin and N-cadherin complex also occurs during synapse formation (Uchida et al., 1996). Interestingly, while we confirmed this complex following immunoprecipitation with β-catenin and N-cadherin antibodies (Figures 1B, C), N-cadherin could not be detected in MET pull-downs (Figure 1A). These data show that β-catenin forms separate complexes with MET and with N-cadherin. Moreover, following HGF stimulation, there is an increase in N-cadherin/β-catenin complex (mean fold change (HGF/PBS): 1.309, 95% CI: [1.018, 1.600] for N-cadherin in β-catenin IP; mean

fold change (HGF/PBS): 1.388, 95% CI: [0.6342, 2.141] for β-catenin in N-cadherin IP; Figure 1D) that complement the reduced MET/β-catenin complex (Figures 1A, B and D).

We next used the PLA assay to examine the proximity of MET/β-catenin in primary cultures of neocortical neurons. At 14DIV, PLA signal was detected in the presence of MET and β-catenin antibodies (Figure 1E), indicating a close proximity between these two proteins. There was a significant effect of treatment (PBS versus HGF) on the magnitude of the PLA signal ($F[1,174] = 9.401$, $p = 0.0025$, Figure 1F). Pairwise analysis revealed that there was no effect for HGF stimulation for 5 minutes (PBS versus HGF: $p^a = 0.8383$, df = 174) but there was a significant reduction in PLA signal after HGF stimulation for 10 minutes ($p^b = 0.0002$, df = 174). Specifically, after stimulation for 10 minutes, there was a ~50% decrease in the density of PLA clusters in HGF- compared to PBS-treated cultures (Figure 1F). The PLA signal returned to pre-stimulation levels 30 minutes following HGF treatment (PBS versus HGF: $p^c = 0.0723$, df = 174, Figure 1F). Together, the co-IP/Western and PLA analyses demonstrate that MET/β-catenin proximity is regulated in an HGF-dependent manner.

In the third set of experiments, we used RNAscope to examine the co-expression of *Met* and *β-catenin* in the mouse neocortex at P14, providing an anatomical context for MET and β-catenin complex in vivo. There was a gradient of *Met* and *β-catenin* co-expression across neocortical layers (Figure 1G). Specifically, in layers II/III, there were many neurons that co-expressed the *Met* and *β-catenin* transcripts (Figure 1G'). In deeper layers, the signal intensity of puncta was greater in co-labeled neurons (Figure

1G''). In both superficial and deep layers, there also were single-labeled *Met* or *β-catenin* pyramidal neurons (Figures 1G', G''). These data indicate that the MET/β-catenin complex resides in subsets of neocortical neurons during the peak period of synapse formation. This heterogeneity in neuronal co-expression may account in part for the disruption of physiological functions in a subset of neocortical synapses after *Met* deletion (Qiu et al., 2011).

HGF increases the synapsin 1/MET complex during synapse development

Following HGF stimulation, β-catenin dissociates from the MET complex. We hypothesized that activation of MET could result in the recruitment of other protein partners into the receptor complex. MET is localized in pre- and post-synaptic compartments, but with predominant enrichment in presynaptic compartments in the developing neocortex (Eagleson et al., 2013) and cultured neocortical neurons. β-catenin also is densely co-localized with presynaptic markers synapsin 1 and neurexin 1 as compared to postsynaptic marker PSD95 in cultured neocortical neurons (Figure 2A). Thus, the experiments here focused on impact of MET receptor activation on presynaptic proteins. In P14 neocortical synaptosomes, synapsin 1 is co-immunoprecipitated with MET (Figure 2B). Further, in contrast to β-catenin, following activation of MET by HGF stimulation for 5 minutes, additional synapsin 1 was recruited to MET complexes (mean fold change (HGF/PBS): 1.804, 95% CI: [1.114, 2.494]; Figure 2B). Consistent with this, the density of the PLA signal generated by MET and synapsin 1 antibody labeling in neocortical neurons *in vitro* was significantly increased (~1.5 fold, p^d = 0.0109, df = 58) following HGF addition, compared with PBS treatment

(Figures 2C and 2D). In contrast to the MET/synapsin 1 complex, MET and synaptophysin 1 do not co-immunoprecipitate under conditions with or without HGF stimulation (Figure 2E). These data suggest that there is an increase in a functional MET/synapsin 1 complex following HGF stimulation.

HGF regulates MET and β-catenin complex through phosphorylation of β-catenin at Y142

Previous reports demonstrated phosphorylation of β-catenin at Y142 in response to HGF in cancer cells and cultured hippocampal neurons (Herynk et al., 2003; Rasola et al., 2007; David et al., 2008; Bhardwaj et al., 2013). Similarly, we found that, following addition of HGF to P14 neocortical synaptomsomes, the level of phosphorylated of β-catenin (Y142) was increased, reaching a peak after 5 minutes, and declining toward pre-stimulation levels by 20 minutes (Figure 3A). Moreover, in cultured neocortical neurons at 14 DIV, the number of immunoreactive puncta, labeled with an antibody that recognizes Y142-phosphorylated β-catenin (Strom et al., 2007; David et al., 2008), significantly increased after HGF treatment for 10 minutes (~2 fold, $p^e = 0.003$, $t = 3.882$, $df = 51$; Figures 3B and 3C). Together, these results indicate that HGF can regulate β-catenin phosphorylation at Y142 in the neocortex during the period of synapse formation.

To address the possibility that phosphorylation of β-catenin at Y142 modulates the extent to which MET and β-catenin functionally interact, neocortical neurons were transfected with wild type β-catenin that can be phosphorylated at Y142 with HGF

383 treatment (Figures 4A and 4B) or a mutant form of β-catenin that cannot be
384 phosphorylated at Y142 (β-cateninY142F) (David et al., 2008). PLA analyses at 14DIV
385 demonstrated that, consistent with our previous data with endogenous β-catenin and
386 MET associated, either directly or indirectly, with transfected β-catenin and MET, this
387 association is down-regulated by HGF (Figure 4C). Quantitative analysis revealed a
388 significant functional association between the construct transfected (wild type β-catenin
389 versus β-cateninY142F) and treatment (PBS versus HGF) on the density of PLA
390 clusters ($F[1,84] = 9.570$, $p = 0.0027$, Figures 4C, D). Pairwise analysis revealed that
391 this effect was due to differences in the PLA signal following HGF stimulation.
392 Specifically, there was no significant difference in the density of PLA clusters between
393 wild type β-catenin and β-cateninY142F in the absence of HGF ($p^f = 0.8269$, $df = 84$,
394 Figures 4C, D), demonstrating that β-cateninY142F still associated in a complex with
395 MET. Following stimulation with HGF, however, there was a significant difference
396 between wild type β-catenin and β-cateninY142F ($p^g = 0.0013$, $df = 84$, Figures 4C, D).
397 Specifically, there was an approximately 70% decrease in the density of PLA clusters in
398 neurons transfected with wild type β-catenin ($p^h = 0.0002$, $df = 84$), but no significant
399 difference in PLA signal in flag-β-cateninY142F-transfected neurons ($p^i > 0.9999$, $df =$
400 84, Figures 4C, D), compared to PBS. These data demonstrate that HGF-stimulated
401 phosphorylation of β-catenin at Y142 is required for the subsequent dissociation of the
402 β-catenin/MET complex. We noted that the transfected β-catenin or β-cateninY142F
403 was distributed in the entire neuron (Figure 4A), but the PLA signals are rarely present
404 in dendrites. The labeling pattern may suggest that HGF stimulation impacts the

405 functional association of MET with transfected β-catenin at presynaptic sites, but we
406 cannot exclude postsynaptic complex interactions.
407
408 **HGF increases the density of Syn-GFP/bassoon and Syn-GFP/PSD95 clusters in**
409 **neocortical neurons**
410 Given the increased MET/synapsin 1 complex following activation of the receptor, we
411 reasoned that HGF/MET signaling might contribute to presynaptic development through
412 an alteration in protein complexes. To address this, we transfected neurons with Syn-
413 GFP, which is a marker of synaptic vesicles, localized at presynapatic sites and axon
414 but not at dendrites (Figure 5B) (Bamji et al., 2003). MET/synaptophysin are not found
415 in the same protein complex. Following transfection, neurons were treated with HGF for
416 10min at 14 DIV. At the end of the treatment period, we categorized Syn-GFP puncta
417 (Figure 5A) according to whether they were: 1) co-labeled with bassoon (Figure 5C), an
418 active zone marker; 2) co-labeled with PSD95 (Figure 5D), a postsynaptic marker; or 3)
419 total labeled Syn-GFP puncta (Syn-GFP), including puncta co-labeled with bassoon or
420 PSD95 and puncta labeled with Syn-GFP alone. Mann-Whitney statistical analyses
421 revealed a significant increase in the density of Syn-GFP puncta co-labeled with
422 bassoon (~2.1-fold, $U(34) = 80$, $p^j = 0.0087$, Figure 5C, E) or with PSD95 (~1.8-fold,
423 $U(34) = 84$, $p^k = 0.0129$, Figure 5D, E) in HGF- compared to PBS-treated cultures. In
424 contrast, there was no significant difference in the density of clusters labeled with Syn-
425 GFP ($U(34) = 103$, $p^l = 0.0633$). We further characterized Syn-GFP puncta co-labeled
426 with bassoon or PSD95, measuring parameters previously shown to be influenced by β-
427 catenin (Sun et al., 2009). There was no significant effect of HGF treatment on the

integrated density (Figure 5F), major length (Figure 5G) or size (Figure 5H) of Syn-GFP puncta, which approximate the size of the synaptic vesicle pool (Sun et al., 2009). Together, these data suggest that HGF promotes the rapid assembly of synaptic vesicles at active zones to increase the formation of nascent synapses, but does not further cause accumulation of synaptic vesicles at existing synaptic sites.

Phosphorylation of β-catenin at Y142 is required for the HGF-induced increase in the density of Syn-GFP/bassoon and Syn-GFP/PSD95 clusters

Previous studies have demonstrated a role for an N-cadherin/β-catenin complex in synaptic vesicle localization at the synapse (Brigidi and Bamji, 2011). Given our data showing that, following HGF stimulation, there is a reduction of the β-catenin/MET complex that is accompanied by an increase in the β-catenin/N-cadherin complex, we wondered whether the HGF-upregulation of Syn-GFP/bassoon and Syn-GFP/PSD95 clusters requires dissociation of the MET/β-catenin complex. To address this, we transfected primary cultures of neocortical neurons with wild type β-catenin or β-cateninY142F, which can form a complex with MET, but does not dissociate from the complex after HGF stimulation. Consistent with our data in untransfected cultures, HGF increased the density of Syn-GFP/bassoon and Syn-GFP/PSD95 clusters in neurons transfected with wild type β-catenin (Figure 6A). In contrast, there was no increase in the density of these clusters in β-cateninY142F-transfected neurons (Figure 6B). Quantitative analysis demonstrated a significant interaction between the construct transfected (wild type β-catenin or β-cateninY142F) and treatment (PBS or HGF) on the density of Syn-GFP/bassoon ($F[1,92] = 8.056$, $p = 0.0056$) and Syn-GFP/PSD95

451 (F[1,116] = 4.141, p = 0.0441) clusters. Pairwise analysis revealed that, in the absence
452 of HGF, there was no significant difference in the density of Syn-GFP/bassoon (p^{v} >
453 0.9999, df = 92, Figure 6C) or Syn-GFP/PSD95 (p^{y} > 0.9999, df = 116, Figure 6D)
454 clusters in neurons transfected with wild type β-catenin or β-cateninY142F. This result
455 suggests that β-cateninY142F does not disrupt Syn-GFP/bassoon or Syn-GFP/PSD95
456 cluster density under conditions in which MET is not stimulated. Following addition of
457 HGF, however, there was a significant increase in the density of Syn-GFP/bassoon (p^{w}
458 = 0.0232, df = 92) and Syn-GFP/PSD95 (p^{z} = 0.0018, df = 116) clusters in neurons
459 transfected with wild type β-catenin, but not in flag-β-cateninY142F-transfected neurons
460 (Syn-GFP/bassoon: p^{x} = 0.3078, df = 92, Syn-GFP/PSD95: p^{aa} > 0.9999, df = 116), as
461 compared to PBS. These results demonstrate that HGF activation of MET promotes an
462 increased density of Syn-GFP/bassoon and Syn-GFP/PSD95 clusters by regulating the
463 MET/β-catenin complex through the phosphorylation of β-catenin at Y142.

Discussion

Many genes have been identified as components of molecular networks involved in ASD risk (Bourgeron, 2009; Pinto et al., 2014). These putative relations are placed in a functional context by examining how interactions at the protein level impact typical and atypical neurodevelopment (Xie et al., 2016). In this context, we demonstrate here a dynamic, ligand-dependent functional interaction, either directly or indirectly, between two proteins encoded by ASD risk genes, *MET* (Campbell et al., 2006; Campbell et al., 2008; Jackson et al., 2009; Thanseem et al., 2010; Zhou et al., 2011; Rudie et al., 2012; Abrahams et al., 2013; Lambert et al., 2014) and *β-catenin* (O'Roak et al., 2012b; O'Roak et al., 2012a). A possible association between MET and WNT/ β-catenin was recently put forth as a contributing mechanism through which neurodevelopmental events impacted in ASD are coordinated (Mullins et al., 2016). Previous reports of functional interactions between MET and β-catenin have focused on transcriptional regulation, in which HGF promotes the phosphorylation of β-catenin at Y142 directly via activating the MET receptor (David et al., 2008), followed by the dissociation of β-catenin from a MET complex and then translocated to the nucleus (Herynk et al., 2003; Rasola et al., 2007; Bhardwaj et al., 2013). We demonstrate a similar modulation of the MET/β-catenin functional interaction by HGF at the neocortical synapse. In contrast to nuclear translocation, however, the released β-catenin is, at least in part, sequestered into N-cadherin complexes, with activated MET receptor recruiting additional synapsin 1 to form functional complexes which may be mediated through other proteins in a complex. In addition to MET, phosphorylation of β-catenin at Y142 could also be induced by other non-receptor tyrosine kinases such as Fer or Fyn tyrosine kinase. This

latter phosphorylation down-regulates the interactions of β-catenin and α-catenin, but does not affect the β-catenin and cadherin adhesive complex, which is controlled by phosphorylation of β-catenin at Y654 (Roura et al., 1999; Piedra et al., 2003; Tai et al., 2007). Independent of HGF/MET signaling, the regulation of cadherin/β-catenin/α-catenin complex by Fer and Fyn tyrosine kinases also contributes to synapse development (Bamji et al., 2006; Arikkath and Reichardt, 2008; Lee et al., 2008).

The dissociation of the MET/β-catenin complex is required for the HGF-induced increase in the density of Syn-GFP/bassoon and Syn-GFP/PSD95 clusters in neocortical neurons. This increase, which is observed over a short assay period of 10 minutes, is suggestive of an increased number of nascent synapses in the presence of HGF and is reminiscent of increased synapse density, defined by synapsin 1 and PSD95 co-localization, in the same culture paradigm after stimulation with HGF for 24 hours (Eagleson et al., 2016). It should be noted that MET signaling also appears to modulate excitatory synapse maturation in the hippocampus and neocortex (Qiu et al., 2014; Peng et al., 2016), such that genetic deletion of *Met* results in premature maturation, assessed morphologically, electrophysiologically and by the increased membrane insertion of AMPA receptor subunits (Qiu et al., 2014). Overexpression of MET in hippocampal neurons or slices in vitro results in both immature spine growth and electrophysiological properties. The data together are consistent with a unique dual role for MET during synapse development - initiating synapse formation at early stages, and maintaining an immature functional state until MET signaling is eliminated. In vivo, MET receptor activation is robust during the period of rapid synapse formation between

510 P7 and 14, but then rapidly falls to near negligible levels by P16 (Eagleson et al., 2016),
511 a time when neocortical synapse are undergoing maturation. While speculative, MET
512 contribution to new synapse formation, followed by a decline to permit maturation, may
513 contribute to the generation of an appropriate number or function of mature excitatory
514 synapses in the developing neocortex. Disruption of MET signaling does increase
515 excitatory drive and synapse maturation, and thus may alter excitation/inhibition
516 balance, a key element contributing to NDDs, including ASD (Rubenstein and
517 Merzenich, 2003; Levitt et al., 2004; Dani et al., 2005; Gogolla et al., 2009; Gatto and
518 Broadie, 2010; Bateup et al., 2013).
519
520 In the current study, we focused on the role of MET/β-catenin complex in
521 modulating presynaptic development. Specifically, HGF increases synaptic vesicles
522 clustering at the active zone and at the synapse through regulation of MET/β-catenin
523 complex by phosphorylation of β-catenin at Y142. We also showed that, under basal
524 culture condition, β-catenin as well as β-catenin Y142F itself could promote synapse
525 formation. This may reflect the role of β-catenin independent of HGF/MET signaling and
526 phosphorylation of β-catenin at Y142 as discussed previously (Arikkath and Reichardt,
527 2008; Sun et al., 2009; Brigidi and Bamji, 2011), as well as the low concentration of
528 HGF in our basal culture condition. The low concentration of HGF may not generate
529 sufficient phosphorylation of β-catenin at Y142 to induce difference between β-catenin
530 and β-catenin Y142F transfected neurons. It should be noted that the regulation of
531 MET/β-catenin complex by HGF may occur at both pre- and post-synaptic sites,
532 because *in vivo*, both β-catenin and MET are also localized at postsynaptic sites in the

neocortex and hippocampus (Phillips et al., 2001; Murase et al., 2002; Eagleson et al., 2013). Thus, the increased alignment of synaptic vesicles at active zone and at synapse induced by HGF could be triggered through regulation of both pre- and post-synaptic MET/β-catenin complexes in the cultured neurons. It also should be noted that MET is localized predominantly in presynaptic compartments, and there is no individual synapse with MET distributed at both pre- and post-synaptic sites in the developing neocortex in vivo (Eagleson et al., 2013). While it awaits formal testing, we favor the hypothesis that the major regulation of MET/β-catenin complexes would occur at the presynaptic site in the developing neocortex *in vivo*. However, we note that, β-catenin and MET have been demonstrated independently to modulate several features of postsynaptic development. For example, β-catenin regulates dendritic morphogenesis**,** dendritic spine density, and postsynaptic structure and function (Murase et al., 2002; Yu and Malenka, 2003; Abe et al., 2004; Yu and Malenka, 2004; Gao et al., 2007; Okuda et al., 2007). Similarly, there is increasing evidence that MET signaling modulates dendritic and spine morphogenesis, as well as the clustering of postsynaptic proteins, including PSD95 (Gutierrez et al., 2004; Lim and Walikonis, 2008; Judson et al., 2010; Finsterwald and Martin, 2011; Judson et al., 2011; Qiu et al., 2014; Peng et al., 2016). Thus, it is plausible that the MET/β-catenin complex, and the regulation of this complex by HGF, may influence different aspects of pre- and postsynaptic development.

The analyses of HGF-induced regulation of MET/β-catenin functional interactions in neocortical neurons *in vitro* raise the issue of defining the cellular and circuit context in which this signaling system may operate *in vivo*. At P14, we found that there are both

co-labeled and single labeled neurons expressing *Met* and *β-catenin* transcripts in layers II-III and V-VI. The double-labeled neurons located superficially are almost entirely intrinsic intratelencephalic cortico-cortical or callosal neurons, where as deep layer MET+ neurons could be both callosal and cortico-fugal in nature. During the active period of synaptogenesis in the mouse neocortex, *Hgf* mRNA is evident mostly in deep layers of the neocortex at P14 (Eagleson et al., 2016). Thus, both ligand and receptor are positioned to modulate MET/β-catenin complexes in subsets of neurons *in vivo*. Determining the specific subpopulation identifies are currently under investigation.

Our current findings are consistent with converging evidence that the developing neocortical synapse is disrupted in ASD, with many ASD risk genes having implicated or demonstrated roles in synapse development and plasticity (Zoghbi, 2003; Garber, 2007; Sudhof, 2008; Zoghbi and Bear, 2012; De Rubeis et al., 2014; Xie et al., 2016). Less progress has been made in understanding the heterogeneity in clinical presentation, which likely reflects the polygenic nature of the disorder. Our data suggest that an understanding of ASD risk at the level of protein functional interactions, including identification of the specific subpopulations of neurons and circuits in which these interactions occur, will provide insight into how such heterogeneity arises. For example, MET expression in the primate brain is enriched in temporal, posterior parietal and occipital regions, with very limited expression in few frontal lobe areas. Neuroimaging studies confirm that the MET promoter risk variant impacts structure and function of circuits in which it is enriched (Rudie et al., 2012). At the cellular level, the RNAscope analyses reveal that a subset of neocortical neurons co-express MET and β-catenin

579 during the peak period of synaptogenesis. This suggests that the biological impact of
580 reducing MET expression, which occurs in ASD and Rett syndrome (Campbell et al.,
581 2007; Voineagu et al., 2011; Plummer et al., 2013), may differentially disrupt the
582 development of subpopulations of neurons, with specific changes being dependent on
583 the specific repertoire of MET-interacting proteins expressed by different neurons and
584 circuits. Advances in multiplex in situ techniques will provide opportunities to more
585 carefully characterize the co-expression of multiple members of the MET interactome,
586 11% of which have been associated with neurodevelopmental disorders (Xie et al.,
587 2016), in discrete neocortical neuron subpopulations.
588
589

590 **References**

591 Abe K, Chisaka O, Van Roy F, Takeichi M (2004) Stability of dendritic spines and
592 synaptic contacts is controlled by alpha N-catenin. Nat Neurosci 7:357-363.
593 Abrahams BS, Arking DE, Campbell DB, Mefford HC, Morrow EM, Weiss LA, Menashe
594 I, Wadkins T, Banerjee-Basu S, Packer A (2013) SFARI Gene 2.0: a community-
595 driven knowledgebase for the autism spectrum disorders (ASDs). Molecular
596 Autism 4:1-1.
597 Arikkath J, Reichardt LF (2008) Cadherins and catenins at synapses: roles in
598 synaptogenesis and synaptic plasticity. Trends in neurosciences 31:487-494.
599 Bamji SX, Rico B, Kimes N, Reichardt LF (2006) BDNF mobilizes synaptic vesicles and
600 enhances synapse formation by disrupting cadherin-beta-catenin interactions.
601 The Journal of cell biology 174:289-299.
602 Bamji SX, Shimazu K, Kimes N, Huelsken J, Birchmeier W, Lu B, Reichardt LF (2003)
603 Role of beta-catenin in synaptic vesicle localization and presynaptic assembly.
604 Neuron 40:719-731.
605 Bateup HS, Johnson CA, Denefrio CL, Saulnier JL, Kornacker K, Sabatini BL (2013)
606 Excitatory/inhibitory synaptic imbalance leads to hippocampal hyperexcitability in
607 mouse models of tuberous sclerosis. Neuron 78:510-522.
608 Beaudoin GM, 3rd, Lee SH, Singh D, Yuan Y, Ng YG, Reichardt LF, Arikkath J (2012)
609 Culturing pyramidal neurons from the early postnatal mouse hippocampus and
610 cortex. Nature protocols 7:1741-1754.

611 Bhardwaj D, Nager M, Camats J, David M, Benguria A, Dopazo A, Canti C, Herreros J
612 (2013) Chemokines induce axon outgrowth downstream of Hepatocyte Growth
613 Factor and TCF/beta-catenin signaling. Frontiers in cellular neuroscience 7:52.
614 Bourgeron T (2009) A synaptic trek to autism. In: Current Opinion in Neurobiology, pp
615 231-234.
616 Bozkaya G, Korhan P, Cokakli M, Erdal E, Sagol O, Karademir S, Korch C, Atabey N
617 (2012) Cooperative interaction of MUC1 with the HGF/c-Met pathway during
618 hepatocarcinogenesis. Mol Cancer 11:64.
619 Brigidi GS, Bamji SX (2011) Cadherin-catenin adhesion complexes at the synapse.
620 Current opinion in neurobiology 21:208-214.
621 Burghy CA, Stodola DE, Ruttle PL, Molloy EK, Armstrong JM, Oler JA, Fox ME, Hayes
622 AS, Kalin NH, Essex MJ, Davidson RJ, Birn RM (2012) Developmental pathways
623 to amygdala-prefrontal function and internalizing symptoms in adolescence. Nat
624 Neurosci 15:1736-1741.
625 Campbell DB, Li C, Sutcliffe JS, Persico AM, Levitt P (2008) Genetic evidence
626 implicating multiple genes in the MET receptor tyrosine kinase pathway in autism
627 spectrum disorder. Autism research : official journal of the International Society
628 for Autism Research 1:159-168.
629 Campbell DB, D'Oronzio R, Garbett K, Ebert PJ, Mirnics K, Levitt P, Persico AM (2007)
630 Disruption of cerebral cortex MET signaling in autism spectrum disorder. Annals
631 of neurology 62:243-250.
632 Campbell DB, Sutcliffe JS, Ebert PJ, Militerni R, Bravaccio C, Trillo S, Elia M, Schneider
633 C, Melmed R, Sacco R, Persico AM, Levitt P (2006) A genetic variant that

disrupts MET transcription is associated with autism. Proceedings of the National Academy of Sciences of the United States of America 103:16834-16839.

Crowell B, Lee GH, Nikolaeva I, Dal Pozzo V, D'Arcangelo G (2015) Complex Neurological Phenotype in Mutant Mice Lacking Tsc2 in Excitatory Neurons of the Developing Forebrain(123). eNeuro 2.

Dani VS, Chang Q, Maffei A, Turrigiano GG, Jaenisch R, Nelson SB (2005) Reduced cortical activity due to a shift in the balance between excitation and inhibition in a mouse model of Rett syndrome. Proceedings of the National Academy of Sciences of the United States of America 102:12560-12565.

David MD, Yeramian A, Dunach M, Llovera M, Canti C, de Herreros AG, Comella JX, Herreros J (2008) Signalling by neurotrophins and hepatocyte growth factor regulates axon morphogenesis by differential beta-catenin phosphorylation. Journal of cell science 121:2718-2730.

De Rubeis S et al. (2014) Synaptic, transcriptional and chromatin genes disrupted in autism. Nature.

DeAngelis T, Morrione A, Baserga R (2010) Mutual interaction and reciprocal down-regulation between c-met and insulin receptor substrate-1. J Cell Physiol 224:658-663.

Eagleson KL, Milner TA, Xie Z, Levitt P (2013) Synaptic and extrasynaptic location of the receptor tyrosine kinase met during postnatal development in the mouse neocortex and hippocampus. The Journal of comparative neurology 521:3241-3259.

656 Eagleson KL, Lane CJ, McFadyen-Ketchum L, Solak S, Wu HH, Levitt P (2016) Distinct
657 intracellular signaling mediates C-MET regulation of dendritic growth and
658 synaptogenesis. Developmental neurobiology. DOI: 10.1002/dneu.22382.
659 Finsterwald C, Martin JL (2011) Cellular mechanisms underlying the regulation of
660 dendritic development by hepatocyte growth factor. The European journal of
661 neuroscience 34:1053-1061.
662 Gao X, Arlotta P, Macklis JD, Chen J (2007) Conditional knock-out of beta-catenin in
663 postnatal-born dentate gyrus granule neurons results in dendritic malformation.
664 The Journal of neuroscience : the official journal of the Society for Neuroscience
665 27:14317-14325.
666 Garber K (2007) Neuroscience. Autism's cause may reside in abnormalities at the
667 synapse. Science 317:190-191.
668 Gatto CL, Broadie K (2010) Genetic controls balancing excitatory and inhibitory
669 synaptogenesis in neurodevelopmental disorder models. Frontiers in synaptic
670 neuroscience 2:4.
671 Gogolla N, Leblanc JJ, Quast KB, Sudhof TC, Fagiolini M, Hensch TK (2009) Common
672 circuit defect of excitatory-inhibitory balance in mouse models of autism. Journal
673 of neurodevelopmental disorders 1:172-181.
674 Gutierrez H, Dolcet X, Tolcos M, Davies A (2004) HGF regulates the development of
675 cortical pyramidal dendrites. Development 131:3717-3726.
676 Hedrick A, Lee Y, Wallace GL, Greenstein D, Clasen L, Giedd JN, Raznahan A (2012)
677 Autism risk gene MET variation and cortical thickness in typically developing

children and adolescents. Autism research : official journal of the International Society for Autism Research 5:434-439.

Herynk MH, Tsan R, Radinsky R, Gallick GE (2003) Activation of c-Met in colorectal carcinoma cells leads to constitutive association of tyrosine-phosphorylated beta-catenin. Clinical & experimental metastasis 20:291-300.

Jackson PB, Boccuto L, Skinner C, Collins JS, Neri G, Gurrieri F, Schwartz CE (2009) Further evidence that the rs1858830 C variant in the promoter region of the MET gene is associated with autistic disorder. Autism research : official journal of the International Society for Autism Research 2:232-236.

Judson MC, Eagleson KL, Levitt P (2011) A new synaptic player leading to autism risk: Met receptor tyrosine kinase. Journal of neurodevelopmental disorders 3:282-292.

Judson MC, Eagleson KL, Wang L, Levitt P (2010) Evidence of cell-nonautonomous changes in dendrite and dendritic spine morphology in the met-signaling-deficient mouse forebrain. The Journal of comparative neurology 518:4463-4478.

Kawas LH, Benoist CC, Harding JW, Wayman GA, Abu-Lail NI (2013) Nanoscale mapping of the Met receptor on hippocampal neurons by AFM and confocal microscopy. Nanomedicine : nanotechnology, biology, and medicine 9:428-438.

Lambert N, Wermenbol V, Pichon B, Acosta S, van den Ameele J, Perazzolo C, Messina D, Musumeci MF, Dessars B, De Leener A, Abramowicz M, Vilain C (2014) A Familial Heterozygous Null Mutation of MET in Autism Spectrum Disorder. Autism research : official journal of the International Society for Autism Research 7:617-622.

Lee SH, Peng IF, Ng YG, Yanagisawa M, Bamji SX, Elia LP, Balsamo J, Lilien J, Anastasiadis PZ, Ullian EM, Reichardt LF (2008) Synapses are regulated by the cytoplasmic tyrosine kinase Fer in a pathway mediated by p120catenin, Fer, SHP-2, and beta-catenin. The Journal of cell biology 183:893-908.

Levitt P, Eagleson KL, Powell EM (2004) Regulation of neocortical interneuron development and the implications for neurodevelopmental disorders. Trends in neurosciences 27:400-406.

Lim CS, Walikonis RS (2008) Hepatocyte growth factor and c-Met promote dendritic maturation during hippocampal neuron differentiation via the Akt pathway. Cellular signalling 20:825-835.

Lu KV, Chang JP, Parachoniak CA, Pandika MM, Aghi MK, Meyronet D, Isachenko N, Fouse SD, Phillips JJ, Cheresh DA, Park M, Bergers G (2012) VEGF inhibits tumor cell invasion and mesenchymal transition through a MET/VEGFR2 complex. Cancer Cell 22:21-35.

Monga SP, Mars WM, Pediaditakis P, Bell A, Mule K, Bowen WC, Wang X, Zarnegar R, Michalopoulos GK (2002) Hepatocyte growth factor induces Wnt-independent nuclear translocation of beta-catenin after Met-beta-catenin dissociation in hepatocytes. Cancer research 62:2064-2071.

Mullins C, Fishell G, Tsien RW (2016) Unifying Views of Autism Spectrum Disorders: A Consideration of Autoregulatory Feedback Loops. Neuron 89:1131-1156.

Murase S, Mosser E, Schuman EM (2002) Depolarization drives beta-Catenin into neuronal spines promoting changes in synaptic structure and function. Neuron 35:91-105.

724 Nakano M, Takagi N, Takagi K, Funakoshi H, Matsumoto K, Nakamura T, Takeo S
725 (2007) Hepatocyte growth factor promotes the number of PSD-95 clusters in
726 young hippocampal neurons. Experimental neurology 207:195-202.
727 Niland S, Ditkowski B, Parrandier D, Roth L, Augustin H, Eble JA (2013) Rhodocetin-
728 alphabeta-induced neuropilin-1-cMet association triggers restructuring of matrix
729 contacts in endothelial cells. Arterioscler Thromb Vasc Biol 33:544-554.
730 O'Roak BJ et al. (2012a) Sporadic autism exomes reveal a highly interconnected
731 protein network of de novo mutations. Nature 485:246-250.
732 O'Roak BJ et al. (2012b) Multiplex targeted sequencing identifies recurrently mutated
733 genes in autism spectrum disorders. Science 338:1619-1622.
734 Okuda T, Yu LM, Cingolani LA, Kemler R, Goda Y (2007) beta-Catenin regulates
735 excitatory postsynaptic strength at hippocampal synapses. Proceedings of the
736 National Academy of Sciences of the United States of America 104:13479-
737 13484.
738 Peng Y, Huentelman M, Smith C, Qiu S (2013) MET receptor tyrosine kinase as an
739 autism genetic risk factor. International review of neurobiology 113:135-165.
740 Peng Y, Lu Z, Li G, Piechowicz M, Anderson M, Uddin Y, Wu J, Qiu S (2016) The
741 autism-associated MET receptor tyrosine kinase engages early neuronal growth
742 mechanism and controls glutamatergic circuits development in the forebrain.
743 Molecular psychiatry. DOI: 10.1038/mp.2015.182.
744 Phillips GR, Huang JK, Wang Y, Tanaka H, Shapiro L, Zhang W, Shan WS, Arndt K,
745 Frank M, Gordon RE, Gawinowicz MA, Zhao Y, Colman DR (2001) The

presynaptic particle web: ultrastructure, composition, dissolution, and reconstitution. Neuron 32:63-77.

Piedra J, Miravet S, Castano J, Palmer HG, Heisterkamp N, Garcia de Herreros A, Dunach M (2003) p120 Catenin-associated Fer and Fyn tyrosine kinases regulate beta-catenin Tyr-142 phosphorylation and beta-catenin-alpha-catenin Interaction. Molecular and cellular biology 23:2287-2297.

Pinto D et al. (2014) Convergence of Genes and Cellular Pathways Dysregulated in Autism Spectrum Disorders. In: The American Journal of Human Genetics, pp 677-694.

Plummer JT, Evgrafov OV, Bergman MY, Friez M, Haiman CA, Levitt P, Aldinger KA (2013) Transcriptional regulation of the MET receptor tyrosine kinase gene by MeCP2 and sex-specific expression in autism and Rett syndrome. Translational psychiatry 3:e316.

Qiu S, Lu Z, Levitt P (2014) MET Receptor Tyrosine Kinase Controls Dendritic Complexity, Spine Morphogenesis, and Glutamatergic Synapse Maturation in the Hippocampus. The Journal of neuroscience : the official journal of the Society for Neuroscience 34:16166-16179.

Qiu S, Anderson CT, Levitt P, Shepherd GM (2011) Circuit-specific intracortical hyperconnectivity in mice with deletion of the autism-associated Met receptor tyrosine kinase. The Journal of neuroscience : the official journal of the Society for Neuroscience 31:5855-5864.

Rasola A, Fassetta M, De Bacco F, D'Alessandro L, Gramaglia D, Di Renzo MF, Comoglio PM (2007) A positive feedback loop between hepatocyte growth factor

receptor and beta-catenin sustains colorectal cancer cell invasive growth. Oncogene 26:1078-1087.

Reshetnikova G, Troyanovsky S, Rimm DL (2007) Definition of a direct extracellular interaction between Met and E-cadherin. Cell Biol Int 31:366-373.

Roura S, Miravet S, Piedra J, Garcia de Herreros A, Dunach M (1999) Regulation of E-cadherin/Catenin association by tyrosine phosphorylation. J Biol Chem 274:36734-36740.

Rubenstein JL, Merzenich MM (2003) Model of autism: increased ratio of excitation/inhibition in key neural systems. Genes, brain, and behavior 2:255-267.

Rudie JD, Hernandez LM, Brown JA, Beck-Pancer D, Colich NL, Gorrindo P, Thompson PM, Geschwind DH, Bookheimer SY, Levitt P, Dapretto M (2012) Autism-associated promoter variant in MET impacts functional and structural brain networks. Neuron 75:904-915.

Smyth LA, Brady HJ (2005) cMet and Fas receptor interaction inhibits death-inducing signaling complex formation in endothelial cells. Hypertension 46:100-106.

Strom A, Bonal C, Ashery-Padan R, Hashimoto N, Campos ML, Trumpp A, Noda T, Kido Y, Real FX, Thorel F, Herrera PL (2007) Unique mechanisms of growth regulation and tumor suppression upon Apc inactivation in the pancreas. Development 134:2719-2725.

Sudhof TC (2008) Neuroligins and neurexins link synaptic function to cognitive disease. Nature 455:903-911.

791 Sun Y, Bamji SX (2011) beta-Pix modulates actin-mediated recruitment of synaptic
792 vesicles to synapses. The Journal of neuroscience : the official journal of the
793 Society for Neuroscience 31:17123-17133.
794 Sun Y, Aiga M, Yoshida E, Humbert PO, Bamji SX (2009) Scribble interacts with beta-
795 catenin to localize synaptic vesicles to synapses. Molecular biology of the cell
796 20:3390-3400.
797 Tai CY, Mysore SP, Chiu C, Schuman EM (2007) Activity-regulated N-cadherin
798 endocytosis. Neuron 54:771-785.
799 Thanseem I et al. (2010) Further evidence for the role of MET in autism susceptibility.
800 Neuroscience research 68:137-141.
801 Tyndall SJ, Walikonis RS (2006) The receptor tyrosine kinase Met and its ligand
802 hepatocyte growth factor are clustered at excitatory synapses and can enhance
803 clustering of synaptic proteins. Cell cycle 5:1560-1568.
804 Uchida N, Honjo Y, Johnson KR, Wheelock MJ, Takeichi M (1996) The catenin/cadherin
805 adhesion system is localized in synaptic junctions bordering transmitter release
806 zones. The Journal of cell biology 135:767-779.
807 Voineagu I, Wang X, Johnston P, Lowe JK, Tian Y, Horvath S, Mill J, Cantor RM,
808 Blencowe BJ, Geschwind DH (2011) Transcriptomic analysis of autistic brain
809 reveals convergent molecular pathology. Nature 474:380-384.
810 Wang D, Li Z, Messing EM, Wu G (2005) The SPRY domain-containing SOCS box
811 protein 1 (SSB-1) interacts with MET and enhances the hepatocyte growth
812 factor-induced Erk-Elk-1-serum response element pathway. J Biol Chem
813 280:16393-16401.

814 Wang F, Eagleson KL, Levitt P (2015) Positive regulation of neocortical synapse
815 formation by the Plexin-D1 receptor. Brain Res 1616:157-165.
816 Xie Z, Li J, Baker J, Eagleson KL, Coba MP, Levitt P (2016) Receptor Tyrosine Kinase
817 MET Interactome and Neurodevelopmental Disorder Partners at the Developing
818 Synapse. Biological psychiatry. DOI: 10.1016/j.biopsych.2016.02.022.
819 Yu X, Malenka RC (2003) Beta-catenin is critical for dendritic morphogenesis. Nat
820 Neurosci 6:1169-1177.
821 Yu X, Malenka RC (2004) Multiple functions for the cadherin/catenin complex during
822 neuronal development. Neuropharmacology 47:779-786.
823 Zeng G, Apte U, Micsenyi A, Bell A, Monga SP (2006) Tyrosine residues 654 and 670 in
824 beta-catenin are crucial in regulation of Met-beta-catenin interactions. Exp Cell
825 Res 312:3620-3630.
826 Zheng L, Baumann U, Reymond JL (2004) An efficient one-step site-directed and site-
827 saturation mutagenesis protocol. Nucleic acids research 32:e115.
828 Zhou X, Xu Y, Wang J, Zhou H, Liu X, Ayub Q, Wang X, Tyler-Smith C, Wu L, Xue Y
829 (2011) Replication of the association of a MET variant with autism in a Chinese
830 Han population. PloS one 6:e27428.
831 Zoghbi HY (2003) Postnatal neurodevelopmental disorders: meeting at the synapse?
832 Science 302:826-830.
833 Zoghbi HY, Bear MF (2012) Synaptic dysfunction in neurodevelopmental disorders
834 associated with autism and intellectual disabilities. Cold Spring Harbor
835 perspectives in biology 4. DOI: 10.1101/cshperspect.a009886.
836

837 **Figure Legends**

838 **Figure 1. MET/β-catenin complexes during synapse development.**

839 (A-C) Representative Western blots of complexes immunoprecipitated from P14 cortical
840 crude synaptosomes using anti-MET (A), anti-β-catenin (B), anti-N-cadherin (C), or
841 control IgG antibody. This experiment was repeated three times using independent
842 synaptosomal preparations. In PBS treated synaptosomes, β-catenin (α-β-cat) and MET
843 (α-MET) are detected in MET and β-catenin, but not control IgG, pull-downs. Similarly,
844 β-catenin and N-cadherin (α-N-cad) are evident in N-cadherin and β-catenin, but not
845 control IgG, pull-downs. MET is not detected in the N-cadherin pull-down. Stimulation of
846 synaptosomes for 5 minutes with HGF results in reduced MET and β-catenin
847 complexes, with a concomitant increased in the β-catenin and N-cadherin complexes
848 (HGF lane versus PBS lane). An anti-phospo-MET antibody (α-pMET) was used to
849 confirm HGF-induced activation of the MET receptor. (D) The fold change of HGF
850 stimulated-group as compared to PBS-stimulated group for each IP is presented as
851 box-and-whisker plots. The line bisecting the box represents the median. The horizontal
852 red dash line indicates unchanged level (1.0) for comparison between HGF and PBS. N
853 = 3 independent Co-IP experiments for each interaction. (E) Representative confocal
854 microscopy images of PLA staining in primary cultures of neocortical neurons at 14DIV
855 following treatment with PBS or HGF for 5, 10 and 30 minutes. Red fluorescent profiles
856 represent regions of PLA signal amplification denoting MET and β-catenin co-
857 localization. For comparison, the total MET immunoreactivity (green fluorescence) in the
858 same field is illustrated. Scale bar = 5 μm (applies to all images in E). (F) Quantitative
859 analysis of the MET/β-catenin PLA signals. Error bars represent standard error of the

mean. N = 30 neurons from 4 independent culturing sessions in each group. **p < 0.01 (HGF versus PBS). (G-G'') Dual RNAscope in situ hybridization for *Met* (red) and *β-catenin* (green) in the P14 mouse cortex. Nuclei were labeled with DAPI (blue) to distinguish the cortical layers. Representative confocal microscopy images show *Met* expression in superficial and deep layers, with *β-catenin* expression across all layers, with more intense labeling in layers V and VI (G). Higher magnification images from superficial (G') and deep (G") cortical layers. Dotted circles in G' and G'' indicate RNAscope-labeled single cells. Arrows in G' and G'' indicate *Met* and *β-catenin* co-labeled cells. Arrowheads indicate *Met* (G') or *β-catenin* (G'') single labeled neurons. Scale bar = 200 μm in G; 25 μm in G'' (applies to G' and G'').

Figure 2. HGF recruits additional synapsin 1 to MET receptor complex.

(A) Quantitative analysis of PLA signals generated with β-catenin alone (β-cat), β-catenin with MET (+ MET), β-catenin with synapsin 1 (+ Syn 1), β-catenin with Neurexin 1 (+ Nxn 1) and β-catenin with PSD95 (+ PSD-95). Error bars represent standard error of the mean, N = 6 - 8 cells from independent cultures for each group. (B) Representative Western blots of complexes immunoprecipitated from P14 cortical crude synaptosomes using an anti-MET or control IgG antibody. This experiment was repeated three times using independent synaptosomal preparations. In PBS treated synaptomsomes, synapsin 1 and MET are detected in the MET, but not IgG, pull-downs. Stimulation of the synaptosomes for 5 minutes with HGF increased the MET/synapsin 1 complex (HGF vs PBS lane). An anti-phospo-MET antibody (α-pMET) was used to confirm HGF-induced activation of the MET receptor. (C) Representative

confocal microscopy images of PLA staining in primary cultures of neocortical neurons at 14DIV following treatment with PBS or HGF for 10 minutes. Red fluorescent profiles represent regions of PLA signal amplification denoting MET and synapsin 1 co-localization. For comparison, the total MET immunoreactivity (green fluorescence) in the same field is illustrated. Scale bar = 5 μm (applies to all images in B). (D) Quantitative analysis of the MET/synapsin 1 PLA signals. Error bars represent standard error of the mean, N = 30 cells from 5 independent cultures in each group. *$p < 0.05$ (HGF versus PBS). (E) Representative Western blots of complexes that were immunoprecipitated from P14 cortical crude synaptosomes using an anti-MET or control IgG antibody. MET are detected in the MET, but not IgG, pull-downs. Stimulation of the synaptosomes for 5 minutes with HGF results in phospho-MET detection in MET pull-downs (HGF vs PBS lane). A single synaptophysin 1 band is readily detected in the input sample, prior to IP. In contrast, the post-immunoprecipitation sample has only non-specific bands in all Co-IP groups, indicating that synaptophysin 1 does not co-immunoprecipitate with MET under these conditions.

Figure 3. HGF promotes phosphorylation of β-catenin at Y142.

(A) Representative Western blots of crude neocortical synaptosomes following stimulation with HGF stimulation for 0, 5, 10 and 20 minutes. This experiment was repeated three times using independent synaptosomal preparations. The level of β-catenin phosphorylated at Y142 (p142-β-cat) increased in the presence of HGF, peaking at 5 minutes. Note the expected increase, followed by a time-dependent decrease, in phospho-MET (pMET) levels in response to HGF. Total levels of β-catenin

(β-cat) and MET are unchanged. (B) Representative confocal microscopy images of primary neocortical neurons at 14 DIV following stimulation for 5 minutes with PBS or HGF (25 ng/ ml). This experiment was repeated in two independent culturing sessions. Note the increase in immunostaining of p142- β-catenin in the presence of HGF. Scale bar = 20 μm (applies to both images in B). (C) Quantitative analysis of the p142- β-catenin clusters. Error bars represent standard error of the mean, N = 26 cells from 2 independent cultures in each group. *$p < 0.05$ (HGF versus PBS).

Figure 4. HGF modulates MET/β-catenin complex via phosphorylation of β-catenin at Y142.

(A) Neurons were transfected with flag-tagged wild type β-catenin (Flag-β-cat). Representative confocal microscopy image of transfected neuron with total flag immunoreactivity (white) was shown. Note that transfected β-catenin was distributed along the entire neuron and processes. Scale bar = 50 μm. (B) Representative confocal microscopy images of Flag-β-cat transfected neurons with total flag (green) and p142-β-catenin immunoreactivity (white). Note the positive immunostaining of p142- β-catenin in the Flag-β-cat transfected neuron with stimulation of HGF. Scale bar = 25 μm. (C) Representative confocal microscopy images of PLA staining of MET and flag in primary cultures of neocortical neurons at 14 DIV following treatment with PBS or HGF for 10 minutes. Neurons were transfected with Flag-β-cat or β-cateninY142F (Flag-β-catY142F) at 5 DIV. Red fluorescent profiles represent regions of PLA signal amplification denoting MET and flag co-localization. For comparison, the total flag immunoreactivity (green fluorescence) in the same field is illustrated. Scale bar = 5 μm

(applies to all images in C). (D) Quantitative analysis of the MET/flag PLA signals. Error bars represent standard error of the mean, N = 22 cells from 3 independent cultures in each group. Note the decrease is PLA signal with HGF in the wild type Flag-β-catY, but no change with HGF in the Flag-β-catY142F condition. **p < 0.01 (HGF versus PBS in Flag-β-cat-transfected group), n.s.: no significance (Flag-β-cat versus Flag-β-catY142F with PBS stimulation, HGF versus PBS in Flag-β-catY142F-transfected group).

Figure 5. MET activation increases the density of Syn-GFP/bassoon and Syn-GFP/PSD95 clusters in neocortical neurons.

(A) Diagram of synaptophysin-GFP (Syn-GFP) cluster assay. Neocortical neurons were transfected with Syn-GFP at 5DIV and treated with PBS or HGF (25 ng/ml) for 10 minutes at 14 DIV. Measurements were made of 1) Syn-GFP/Bassoon (a marker of the active zone) co-labeled clusters, 2) Syn-GFP/PSD95 (a marker of the postsynaptic density) co-labeled clusters, and 3) clusters labeled with Syn-GFP along axon (with active zone and synapse included). (B) Representative confocal microscopy image of Syn-GFP (green) transfected neurons. Note Syn-GFP clusters are present along axons but not dendrites. Scale bar = 50 μm. (C-D) Representative confocal microscopy images of Syn-GFP (green), bassoon (red) and PSD95 (magenta) immunoreactivity in neocortical neurons. White arrows indicate clusters co-labeled with Syn-GFP/bassoon (C) or Syn-GFP/PSD95 (D). Scale bar = 5 μm (applies to all images in C and D). (E-H) Quantitative analysis of the density (E), integrated density (F), major length (G) and size (H) of Syn-GFP clusters. Each parameter was normalized in each culturing session to the mean value of Syn-GFP clusters in the PBS treated group. Error bars represent

standard error of the mean, N = 18 cells from 3 independent cultures in each group. Increases in co-labeling of pre/postsynaptic markers are evident following HGF stimulation. *p < 0.05, **p < 0.01 (HGF versus PBS).

Figure 6. Phosphorylation of β-catenin at Y142 is required for the HGF-induced increase in Syn-GFP/bassoon and Syn-GFP/PSD95 clusters.

(A-B) Representative confocal microscopy images of Syn-GFP (green), bassoon (red), PSD95 (magenta) and flag (blue) immunoreactivity in neocortical neurons at 14 DIV after treatment with PBS or HGF (25 ng/ml) for 10 minutes. The neurons were co-transfected with Syn-GFP and either flag-β-catenin (A) or flag-β-cateninY142F (B) plasmids at 5DIV. White arrows indicate clusters co-labeled with Syn-GFP/bassoon (upper panels) or Syn-GFP/PSD95 (lower panels). Scale bar = 5 μm (applies to all images in A and B). (C-D) Quantitative analysis of the density of Syn-GFP/bassoon (C) and Syn-GFP/PSD95 co-labeled clusters in β-catenin (β-cat)- or β-cateninY142F (β-catY142F)- transfected neurons. Each parameter was normalized in each culturing session to the mean value of Syn-GFP clusters in the PBS treated group. Error bars represent standard error of the mean, N = 24 cells from 3 independent culturing sessions for bassoon co-labeling assay, N =30 cells from 3 independent culturing sessions for PSD95 co-labeling assay. Note the inability to phosphorylate Y142 residue following HGF treatment results in no change in co-labeling of pre/postsynaptic markers. *p < 0.05, **p < 0.01 (HGF versus PBS).

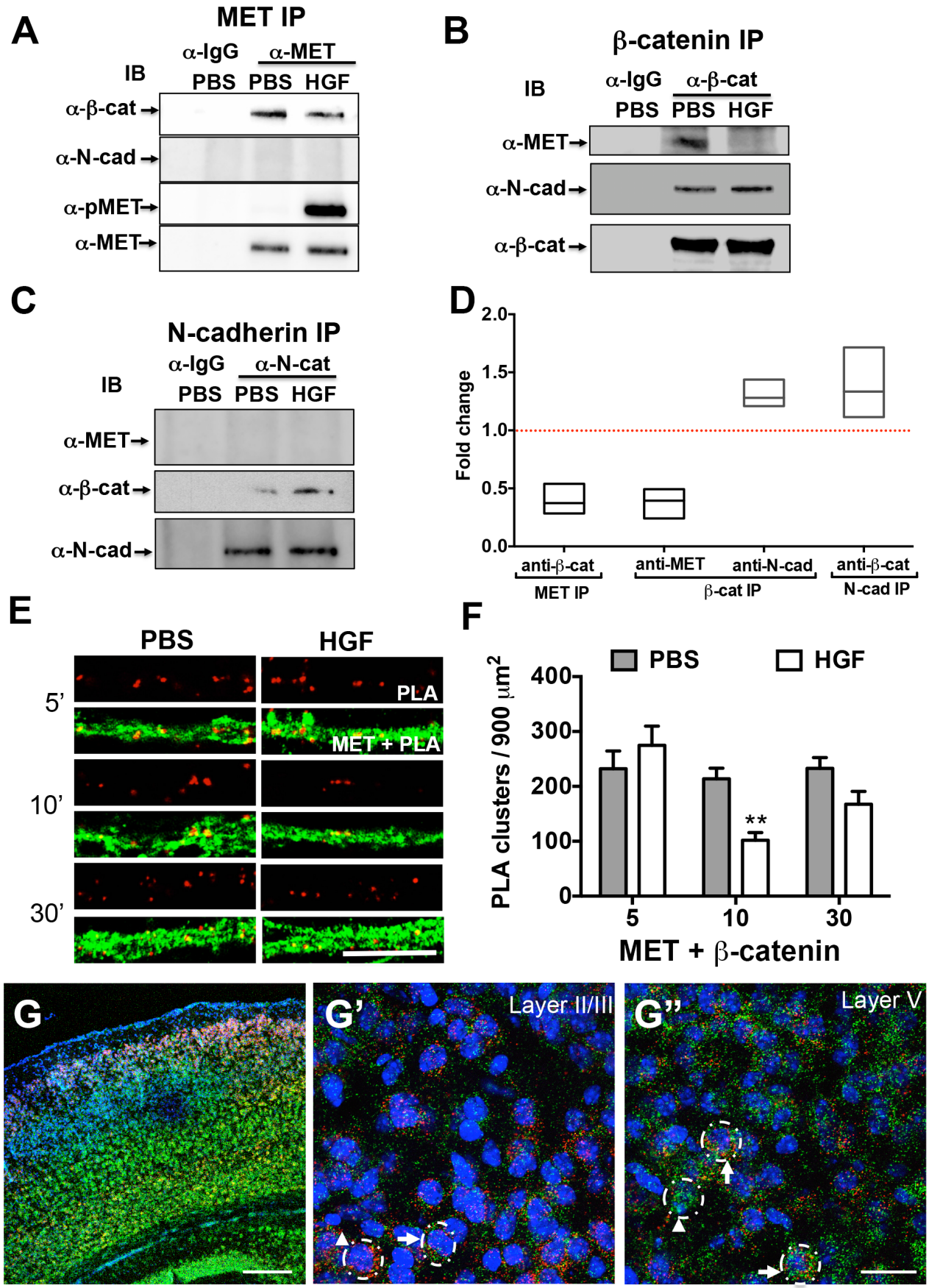

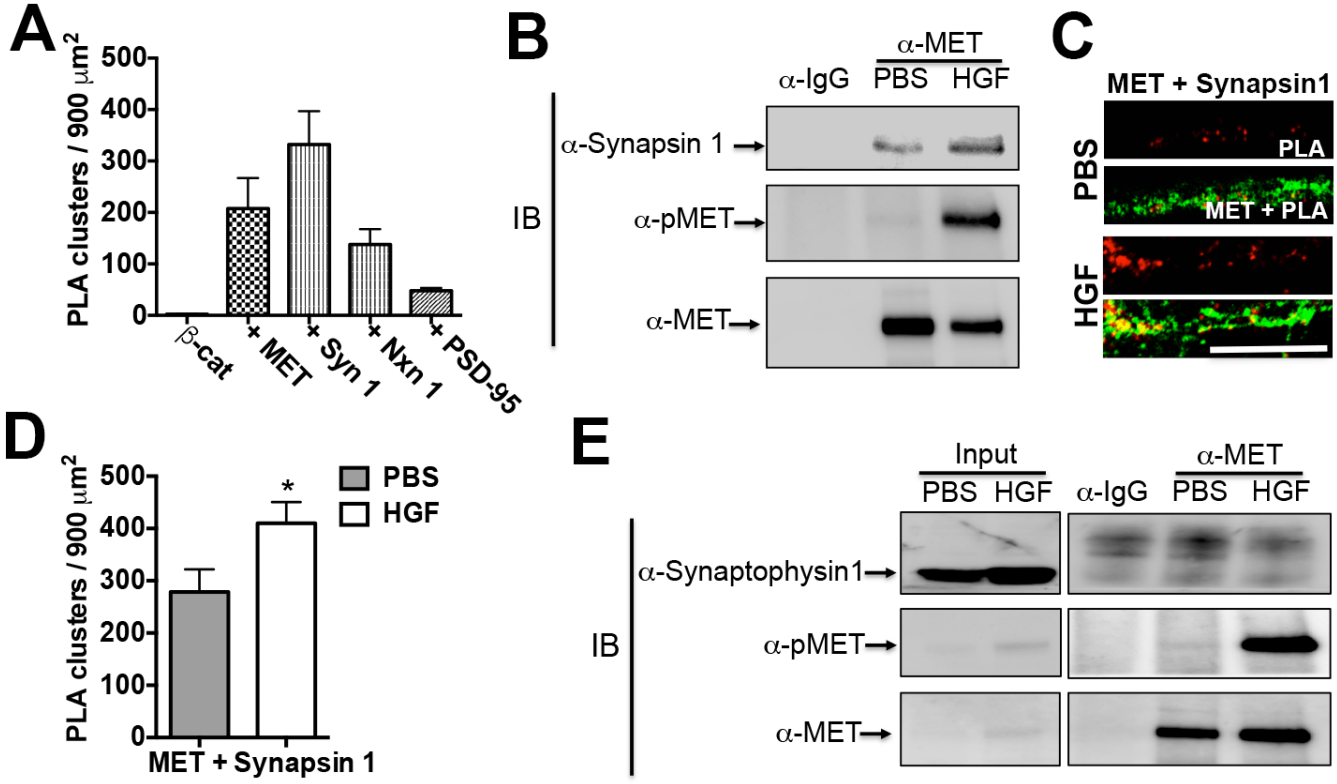

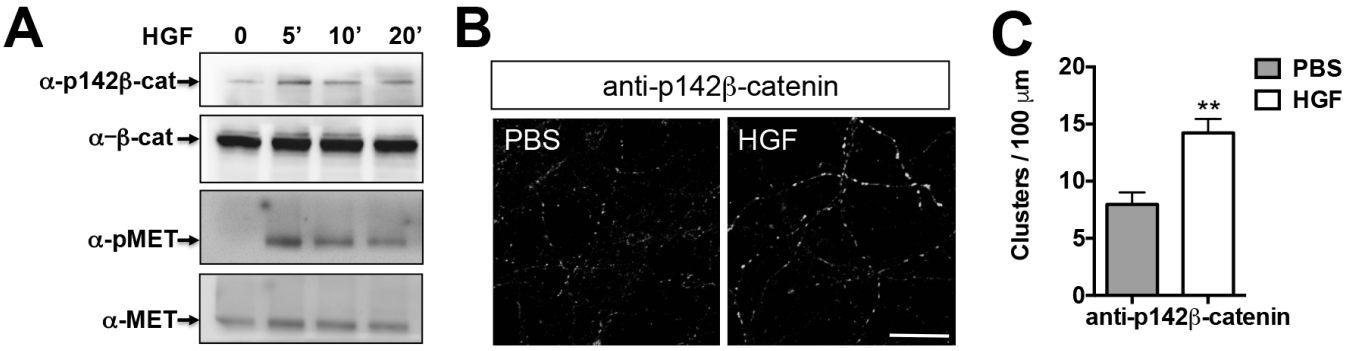

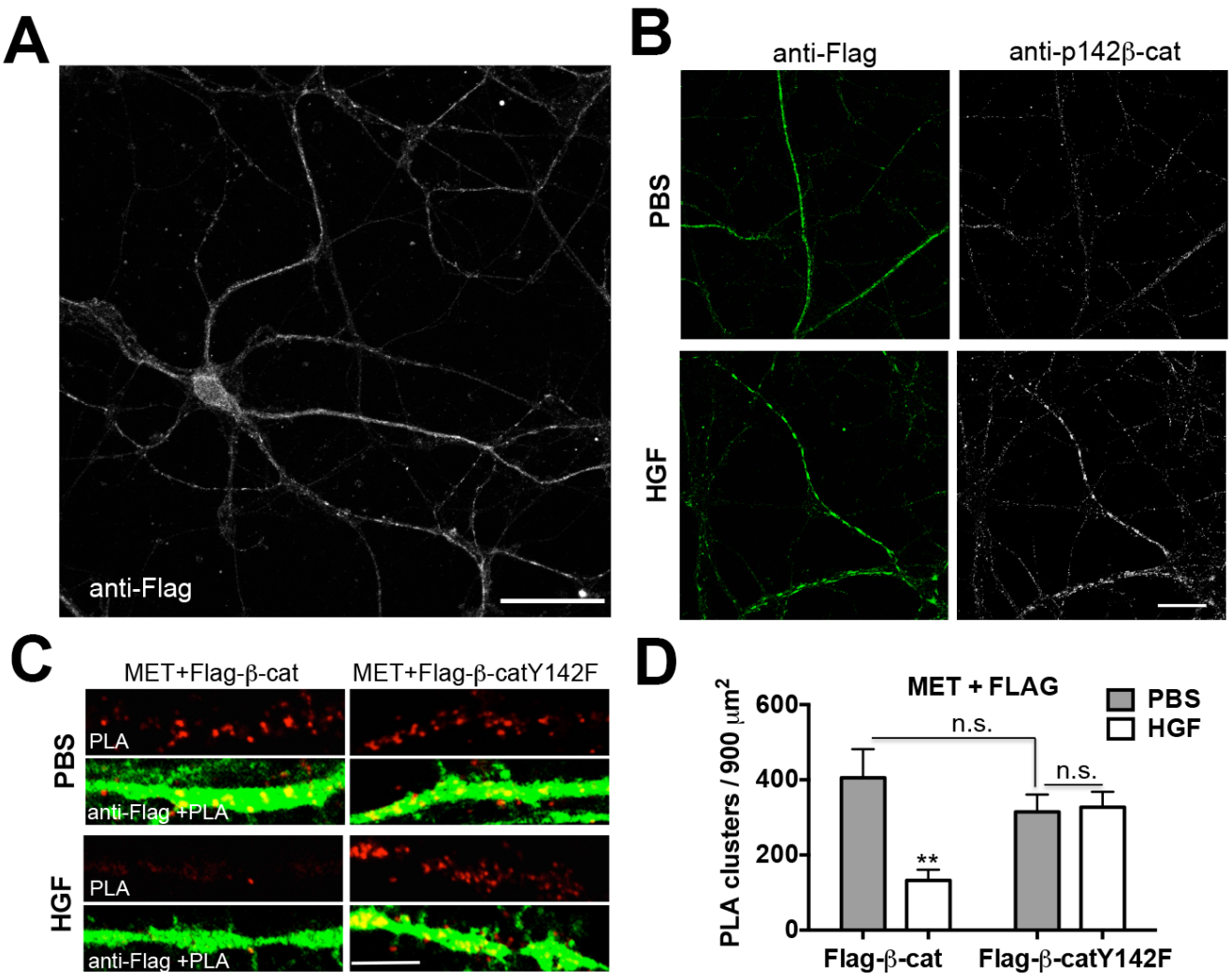

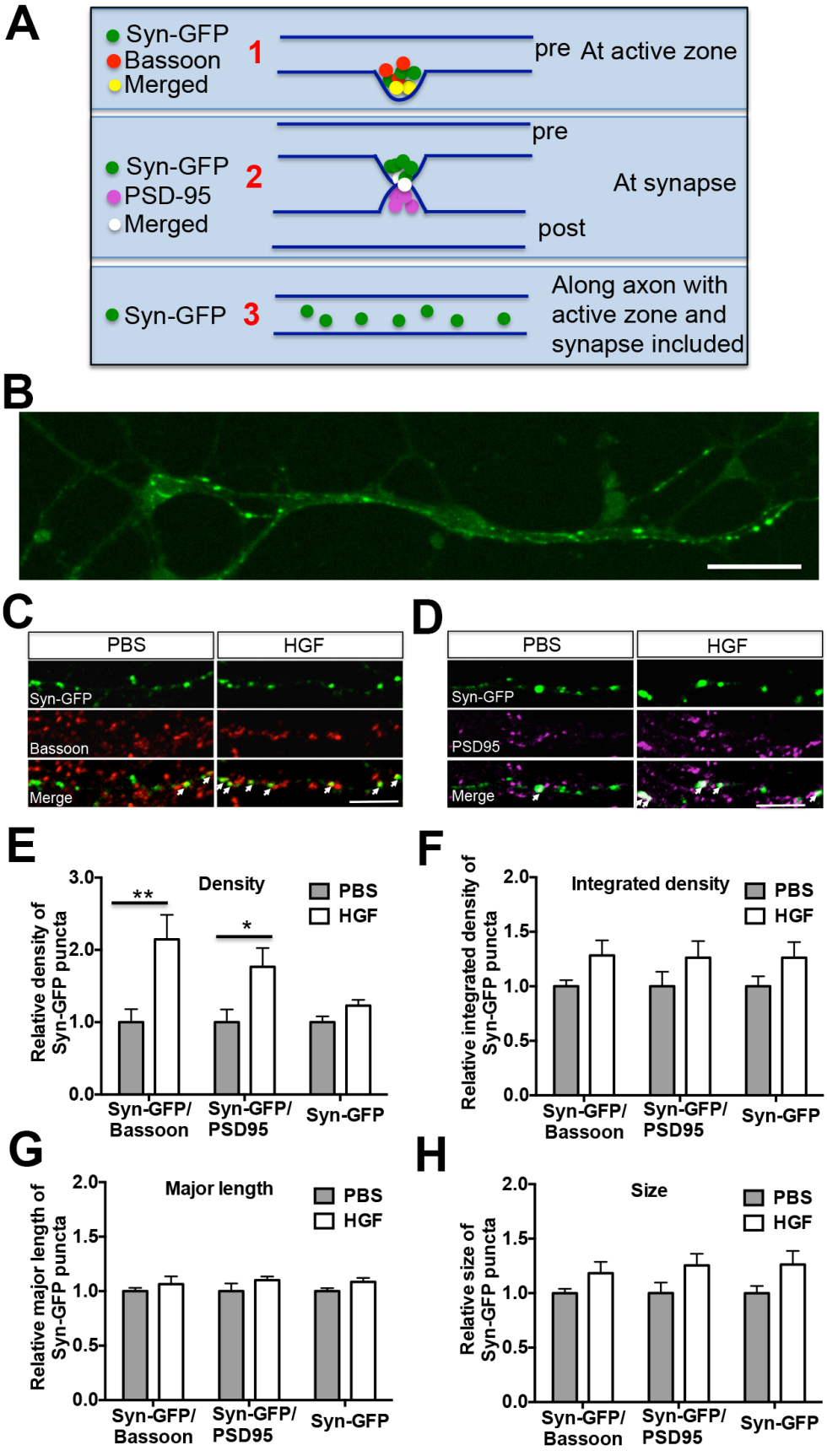

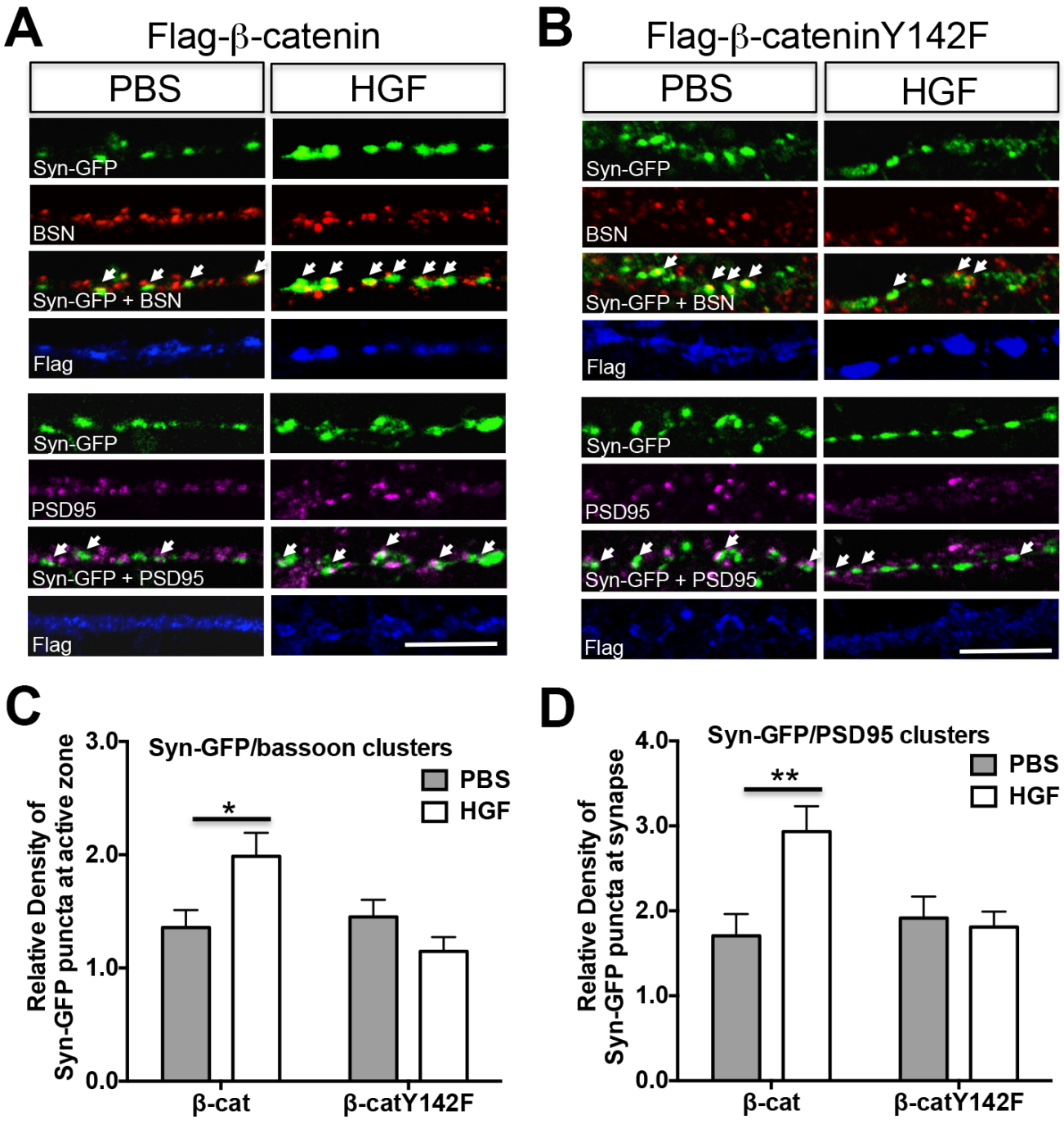

Table 1 Statistical table

Figures	Comparisons	Label	Data Structure	Type of Test	Power
Figure 1F	PBS vs HGF (5 min)	a	Normal distribution after transformation	2-way ANOVA Bonferroni's multiple comparisons test	0.26
	PBS vs HGF (10 min)	b			1.00
	PBS vs HGF (30 min)	c			0.93
Figure 2C	PBS vs HGF	d	Non-normal distribution	Mann Whitney test	0.99
Figure 3C	PBS vs HGF	e	Normal distribution	Unpaired t test with Welch's correction	1.00
Figure 4D	β-catenin vs β-catenin Y142F PBS treatment)	f	Normal distribution after transformation	2-way ANOVA Bonferroni's multiple comparisons test	0.17
	β-catenin vs β-catenin Y142F HGF treatment)	g			1.00
	PBS vs HGF (β-catenin transfection)	h			1.00
	PBS vs HGF (β-catenin Y142F transfection)	i			0.01
Figure 5E	PBS vs HGF (Syn-GFP/Bassoon)	j	Non-normal distribution	Mann Whitney test	0.99
	PBS vs HGF (Syn-GFP/PSD95)	k	Non-normal distribution	Mann Whitney test	0.99
	PBS vs HGF (Syn-GFP)	l	Non-normal distribution	Mann Whitney test	0.94
Figure 5F	PBS vs HGF (Syn-GFP/Bassoon)	m	Non-normal distribution	Mann Whitney test	0.94
	PBS vs HGF (Syn-GFP/PSD95)	n	Non-normal distribution	Mann Whitney test	0.78
	PBS vs HGF (Syn-GFP)	o	Non-normal distribution	Mann Whitney test	0.82
Figure 5G	PBS vs HGF (Syn-GFP/Bassoon)	p	Non-normal distribution	Mann Whitney test	0.90
	PBS vs HGF (Syn-GFP/PSD95)	q	Non-normal distribution	Mann Whitney test	0.75
	PBS vs HGF (Syn-GFP)	r	Normal distribution	Unpaired t test with Welch's correction	0.92
Figure 5H	PBS vs HGF (Syn-GFP/Bassoon)	s	Non-normal distribution	Mann Whitney test	0.91
	PBS vs HGF (Syn-GFP/PSD95)	t	Non-normal distribution	Mann Whitney test	0.90
	PBS vs HGF (Syn-GFP)	u	Non-normal distribution	Mann Whitney test	0.88
Figure 6C	β-catenin vs β-catenin Y142F PBS treatment, Syn-GFP/Bassoon)	v	Normal distribution after transformation	2-way ANOVA Bonferroni's multiple comparisons test	0.00
	PBS vs HGF (β-catenin transfection, Syn-GFP/Bassoon)	w			0.98
	PBS vs HGF (β-cateninY142F transfection, Syn-GFP/Bassoon)	x			0.69
Figure 6D	β-catenin vs β-catenin Y142F PBS treatment, Syn-GFP/PSD95)	y	Normal distribution after transformation	2-way ANOVA Bonferroni's multiple comparisons test	0.00
	PBS vs HGF (β-catenin transfection, Syn-GFP/PSD95)	z			1.00
	PBS vs HGF (β-cateninY142F transfection, Syn-GFP/PSD95)	aa			0.00

Note: To meet the assumption of normality, the data of figures 1F, 4D and 6C were transformed with square root, and the data of figure 6D were transformed with natural logarithm. The normality of the data was tested using D'Agostino & Pearson omnibus normality test.

1. β-catenin interacts with N-Cadherin, SV proteins, and either directly or in a complex with the MET receptor

2. Addition of HGF activates MET, causing phosphorylation of β-catenin Y^{142}, and resulting in MET/β-catenin complex dissociation and an increase in MET and synapsin 1 interactions directly or in a complex. The activation of MET results in new synapse formation.